Advance View
https://doi.org/10.3354/meps13367

MARINE ECOLOGY PROGRESS SERIES
Mar Ecol Prog Ser

Available online:
June 24, 2020

Contribution to the Theme Section: 'Latest advances in research on fish early life stages'

Changing with the tides: fine-scale larval fish prey availability and predation pressure near a tidally modulated river plume

Kelsey Swieca[1,2,*], Su Sponaugle[1,2], Christian Briseño-Avena[2,3], Moritz S. Schmid[2], Richard D. Brodeur[4], Robert K. Cowen[2]

[1]Department of Integrative Biology, Oregon State University, Corvallis, Oregon 97331, USA
[2]Hatfield Marine Science Center, Oregon State University, Newport, Oregon 97365, USA
[3]Department of Environmental and Ocean Sciences, University of San Diego, San Diego, California 92110, USA
[4]National Oceanic and Atmospheric Administration, Northwest Fisheries Science Center, Newport, Oregon 97365, USA

ABSTRACT: Tidally controlled river plumes form distinct frontal boundaries that can alter the spatial distributions of larval fishes and their planktonic prey and predators. Variable in nature, they may expose larval fishes to different trophic environments over small spatio-temporal scales, with unknown consequences for survival and recruitment. In the northern California Current, the Columbia River Plume is strongly influenced by twice-daily freshwater injections that create a highly dynamic coastal environment. Using the *In situ* Ichthyoplankton Imaging System, we examined changes in the fine-scale horizontal and vertical distributions of larval fishes, their prey, and their predators over space and time (ebb/flood tide). In total, 6095 fish larvae and ~1.5 million prey/predator zooplankton were imaged and measured. Plume regions provided substantially higher concentrations of prey and enhanced spatial overlap between larval fishes and their prey relative to oceanic waters. The functionality of river plumes as a refuge from predators was less clear. Predator concentrations were also higher in plume regions, but overlap with larval fishes was taxon-specific and varied with the tide. Notably, regions of high zooplankton concentrations did not necessarily confer high spatial overlap on small scales (meters vertical, kms horizontal) relevant to trophic interactions. Surface salinity and chlorophyll *a* were the most important factors influencing the spatial overlap of zooplankton with larval fishes. In the vicinity of river plumes, larval fishes experience a diversity of unique prey and predator fields over short spatio-temporal scales, which likely contribute to variable growth and mortality patterns at much finer scales than previously thought.

KEY WORDS: Larval fish · Trophic interactions · River plumes · Fine scale · Zooplankton distributions

1. INTRODUCTION

Growth, survival, and recruitment of the critical early life stages of fishes is contingent upon their ability to find food and avoid predation in a physically and biologically heterogeneous environment (Bailey & Houde 1989, Houde 2008). Consequently, the spatio-temporal distributions of prey and predator zooplankton taxa can significantly influence fish population dynamics. Spatial variability in plankton distributions is often attributed to physical gradients in density, temperature, and/or salinity that vary over a wide range of spatial and temporal scales (Graham et al. 2001, Benoit-Bird & McManus 2012, Acha et al. 2015). When abrupt, these gradients can concentrate zooplankton and larval fishes (Grimes & Finucane 1991, Morgan et al. 2005, Munk 2007), creating regions of intensified biologi-

*Corresponding author: swiecak@oregonstate.edu

cal interaction that may disproportionately affect larval fish survival.

Physical features that aggregate prey resources are thought to allow larval fishes to grow quickly and increase survival through their most vulnerable life stages (Lasker 1975). High prey availability typically leads to high feeding success, fast growth, and large size-at-age of larvae (Sponaugle et al. 2009, Pepin et al. 2015). Consequently, oceanographic features that concentrate plankton may lead to heightened recruitment success (Lasker 1975, Shulzitski et al. 2015, 2016). However, this may not always be the case, as the same features that aggregate prey and enhance larval fish feeding also typically concentrate known larval fish predators, especially gelatinous zooplankton (Purcell & Arai 2001, Bakun 2006, McClatchie et al. 2012, Luo et al. 2014). The potentially confounding effects of increased predator abundances are not well understood, due, in part, to the difficulty of sampling fragile gelatinous taxa with traditional net-based techniques. Detailed studies on the fine-scale spatial distributions of larval fishes, their prey, and their predators are needed to understand the mechanisms of larval success and relationships to physical processes.

In many coastal ecosystems, riverine discharge into the ocean creates a shallow, low-salinity, high-turbidity plume that is marked by sharp physical gradients at the plume fronts. Characterized by density discontinuities and hydrodynamic convergence, plume fronts have been shown to aggregate phyto-, zoo-, and ichthyoplankton in a variety of systems including the Gulf of Mexico (Grimes & Finucane 1991, Govoni 1997), Chesapeake Bay (Reiss & McConaugha 1999, Roman et al. 2005), the Gulf of Ancud (Castro et al. 2011), the Sea of Japan (Watanabe et al. 2014), and the Columbia River in the northern California Current (NCC; Morgan et al. 2005, Peterson & Peterson 2008). River plumes are important habitats for larval fishes, and several studies have demonstrated increased encounter rates leading to higher feeding success in larval fish associated with a plume compared to their non-plume-associated conspecifics (e.g. Govoni & Chester 1990, Govoni 1997, Lochmann et al. 1997). Through the accumulation and retention of zooplankton, the location of plume fronts may play an important role in fish population dynamics.

While plume fronts can alter the spatial distributions of zooplankton and are suspected to influence larval fish survival, they are highly variable and often ephemeral in nature. This is particularly true for tidally modulated river plumes where once- or twice-daily freshwater injections modify the strength and location of plume fronts (Acha et al. 2015). One such plume is the Columbia River Plume (CRP) in the NCC. The NCC is oceanographically complex and characterized by dynamic wind-driven upwelling and downwelling processes that support a dense planktonic community (Peterson & Miller 1975). Within the NCC, the Oregon–Washington coastal ecosystem is further complicated by significant freshwater inputs from the second largest runoff river in the USA, the Columbia River (Federal Columbia River Power System; https://www.bpa.gov/news/pubs/GeneralPublications/edu-The-Federal-Columbia-River-Power-System-Inside-Story.pdf). Here, riverine outflow is modulated by large tides that create a plume that varies in volume from 2 to 11 × 10^{10} m^3 (Hickey et al. 1998), is typically on the order of 20 m deep (Bowman 1988), and can extend hundreds of kilometers beyond the continental shelf (García Berdeal et al. 2002, Hickey et al. 2005). The plume region within 50 km of the river mouth is particularly dynamic and varies over small spatial and temporal scales as a result of twice-daily tidal pulses that modify the plume structure (Horner-Devine et al. 2009). At peak ebb tide, the outflow velocity can exceed 3 m s^{-1}, creating strong frontal gradients that have been shown to transport zooplankton off the continental shelf at a rate 5 times faster than typical wind-driven transport (Horner-Devine et al. 2009, Peterson & Peterson 2009). During coastal upwelling events, the plume is diverted southward where it has a longer residency time and is characterized as a far-field 'aged' plume (Horner-Devine et al. 2009).

In systems such as the CRP, fronts are often defined by and sampled along their visually observable surface discontinuity that marks the vertical plume front (Grimes & Finucane 1991, Morgan et al. 2005). However, frontal boundaries occur along both the vertical and horizontal margins, and because plumes are shallow features, the frontal gradient along their horizontal plane is often much larger than the vertical gradient. In the CRP, the formation of distinct vertical and horizontal fronts can change the spatial distributions of zooplankton and may be important features structuring zooplankton communities. Where strong vertical fronts have been shown to aggregate plankton along the leading edge of the plume, strong horizontal gradients are thought to vertically compress phyto- and zooplankton beneath the plume. For example, in the absence of plume waters, zooplankton tend to aggregate in the upper 25 m of the water column, but when the plume is present, zooplankton aggregate at 10 m depth beneath the base of the plume (Peterson & Peterson 2008, 2009).

The Columbia River and its associated plume are a biological hotspot in the Northeast Pacific Ocean.

Not only does this region support many important marine fisheries, including Dungeness crab *Cancer magister* and the largest runs of Pacific salmon (*Oncorhynchus* spp.) in the continental USA, it also serves as an important spawning and nursery habitat for the northern stock of northern anchovy *Engraulis mordax* (Richardson 1981, Emmett et al. 1997, 2005, 2006). In contrast to many other riverine dominated coastal systems, intense hydroelectric regulation of the Columbia River creates artificially high summer flows resulting in a dominant and year-round influence on NCC waters (Henderikx Freitas et al. 2018). Thus, the CRP is a particularly useful system to study how river plumes influence the spatial distributions of zooplankton communities and how those spatial distributions may impact larval fish trophic interactions and population dynamics.

While decades of work have demonstrated that river plumes serve an important role in structuring coastal ecosystems, the physical effects of tidally controlled river plumes on zooplankton spatial distributions, larval fish trophic interactions, and ultimately survival remain poorly understood. This is likely due to the highly dynamic nature of river plumes and the inability of many traditional sampling techniques to resolve both the vertical and horizontal plume margins and fine-scale biological processes. Elucidating these requires high-resolution sampling that can be achieved with underwater imaging, where, with recent technological advancements, data are collected at the scale of an individual larva. We used the high-resolution *In situ* Ichthyoplankton Imaging System (ISIIS) coupled with state-of-the-art machine learning techniques to investigate the fine-scale spatial distribution of larval fishes, their prey, and their predators in the CRP over space (inshore versus offshore) and time (through the progression of a tidal series). Our goal was to measure how various zooplankton and larval fish distributions respond to changes in physical variables. By examining individuals of a diversity of taxonomic groups over time and space, we aimed to determine the degree to which larval fishes overlap with their prey and predators in this dynamic system.

2. MATERIALS AND METHODS

2.1. Data collection

Towed *in situ* imagery data were collected in the NCC just south and offshore of the Oregon–Washington state boundary aboard the NOAA Fisheries RV 'Bell M. Shimada,' as part of the NOAA Northwest Fisheries Science Center Pre-Recruitment Survey (Brodeur et al. 2019). Sampling occurred during daylight hours (08:00–19:00 h PDT) on 23–24 June 2016, and included 2 sequential 25 km cross-plume (parallel to the coastline) transects 10 km offshore of the Columbia River mouth and one 60 km cross-shelf transect south of the river mouth (perpendicular to the coastline), which was split into inshore and offshore sections for further analyses, to capture the plume influence nearshore (Fig. 1A). During the former transect, we transited the same cross-plume line through the progression of the Columbia River ebb-flood tide series (Fig. 1C). The imager was towed at a speed of 2.5 m s^{-1} in a tight undulating fashion from the surface to 100 m depth or within a few meters of the seafloor in shallower regions. Each undulation provided 2 quasi-vertical profiles of the water column. Our sampling resulted in 76 full undulations or 152 quasi-vertical profiles.

2.2. ISIIS

ISIIS (Cowen & Guigand 2008) is a towed, low turbulence, high-resolution *in situ* shadowgraph imaging system. It has a large sampling volume (150–185 l s^{-1}) and is capable of capturing and quantifying both rare plankters, like larval fishes, and their more abundant prey and predators. Additionally, its large field of view (13 × 13 × 50 cm) allows the system to image fragile gelatinous taxa (McClatchie et al. 2012, Luo et al. 2014, 2018), which can be important prey and predators of larval fishes but are difficult to enumerate with traditional net-based sampling techniques (Fig. 2). Sensors on ISIIS include a CTD (Sea-Bird SBE 49 FastCAT), dissolved oxygen (Sea-Bird 43), chlorophyll *a* (chl *a*) fluorescence (Wetlabs FLRT), and photosynthetically active radiation (E_{PAR}; Biospherical QCP-2300). Data from ISIIS are transferred via fiber optic cable to a ship-board computer where images are time-stamped and stored. Imagery data are processed, trained, and tested for automated classification following protocols detailed by Luo et al. (2018). These methods are briefly described below.

2.2.1. Image processing

ISIIS files (AVI stacks) were parsed into single frames and flat-fielded to subtract background noise using a *k*-harmonic means clustering algorithm. Individual plankters, known as regions of interest, were

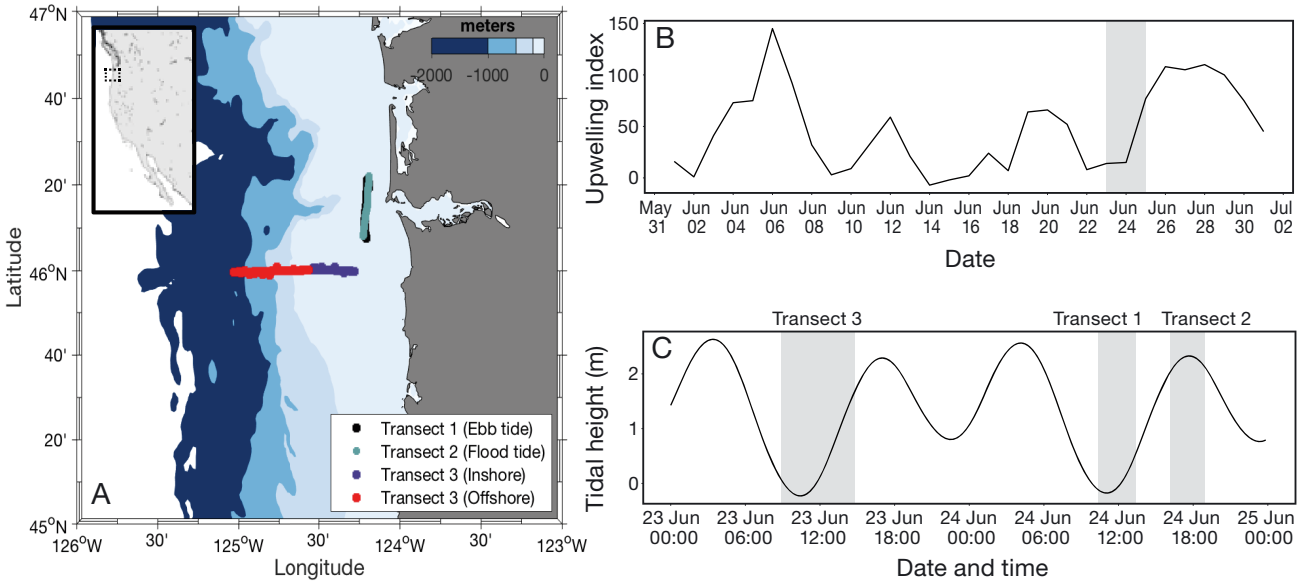

Fig. 1. (A) Study area, showing the 2 cross-plume transects and the cross-shelf transect in relation to the mouth of the Columbia River on 23–24 June 2016. Depth contours are the 200, 500, 1000, and 2000 m isobaths. (B) Bakun upwelling index values for 45° N during the month that sampling occurred, with the grey box highlighting our sampling dates. (C) Tidal height estimates (meters above Mean Lower Low Water) for Astoria, Oregon (CoOp, National Ocean Service, NOAA, Station 9349040). Grey shaded regions indicate sampling periods during the transects (shown in A). Times are in Pacific Daylight Time (PDT)

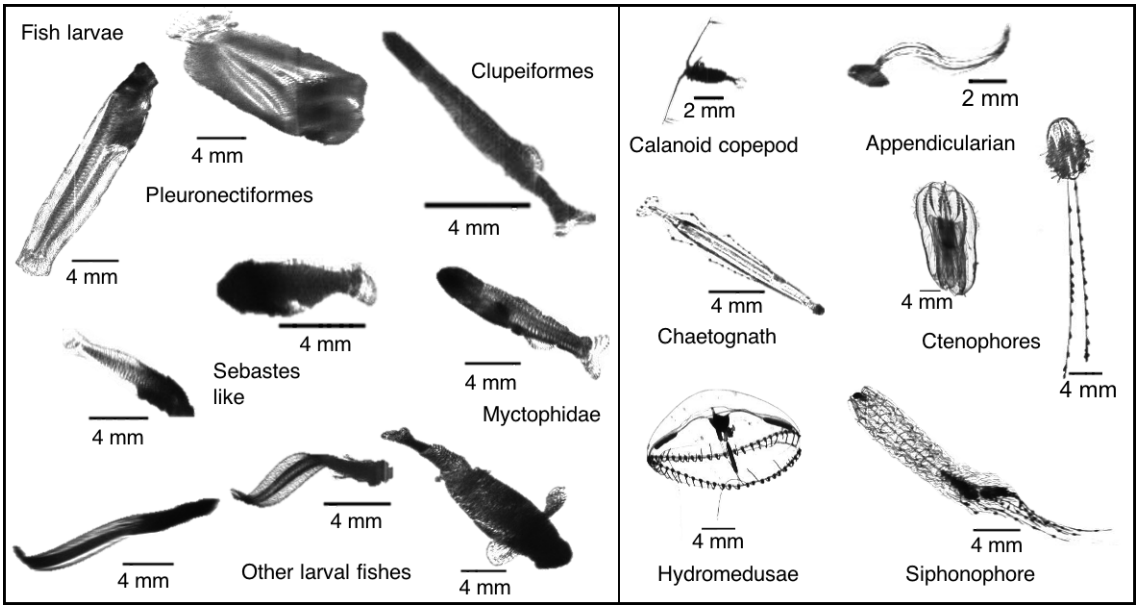

Fig. 2. Images of representative plankton taxa taken by the *In situ* Ichthyoplankton Imaging System (ISIIS) in the northern California Current

detected, segmented from the full frame, assigned a unique name identifier (including a detailed time stamp), and saved as jpg files. Each jpg file contains an individual plankter and will hereafter be referred to as a vignette.

2.2.2. Classification training

A sparse convolutional neural network (sCNN) was used for automated classification of vignettes (single organism images) into taxa categories. sCNNs are

state-of-the-art for the automated identification of *in situ* plankton imagery (Graham 2015, LeCun et al. 2015, Luo et al. 2018). The sCNN is a deep learning tool and was trained using 'SparseConvNets' with 'Fractional Max-Pooling' (Graham 2015) with a customized NCC training library that consisted of 161 categories including phyto-, zoo-, and ichthyoplankton, particles, and noise artifacts (e.g. bubbles at the surface; Table S1 in the Supplement at www.int-res.com/articles/suppl/m13367_supp.pdf). This training library was built by extracting and manually identifying 51 870 vignettes from the entire NCC imagery collection (including the 3 transects analyzed in this study) to accurately capture the diversity of organisms in our sampling region. Both clear and noisy images were included to account for the different water masses sampled, and training of the sCNN continued until an error rate of ≤5% at 400 epochs was attained. An epoch is when the entire dataset is passed though the sCNN once, and the weights, which contain the information that the CNN learned during that epoch, are updated.

The sCNN assigned 161 probabilities to each vignette, indicating to which one of the 161 categories the vignette likely belonged. The category with the highest probability was selected as the predicted identification. Following automated classification, the 161 categories were mapped onto 72 final groups due to the consolidation of multiple categories of the same taxa that needed to be kept separate for automated classification because of differences in orientation, life-stage, or size (Table S1).

2.2.3. Classification testing

Filter-thresholding (*sensu* Faillettaz et al. 2016, Schmid et al. 2020) was applied to remove low-confidence vignettes using a LOESS model. The model calculates a probability threshold cutoff for 90% classification precision at the broader group level. Vignettes with a maximum probability of less than or equal to the calculated cutoff for their category were re-classified as 'unknown' (Table S1). Applying this thresholding reduces the occurrence of false positive identifications substantially. Prediction of true spatial distributions is still possible after removing low classification confidence vignettes (Faillettaz et al. 2016).

The final classification pipeline performance was evaluated using a confusion matrix (Hu & Davis 2006, Tharwat 2018). We compared the results of 86 681 randomly selected and manually identified vignettes to their automated predicted classification from the sCNN. This provided a number of true positives (TPs), false positives (FPs), and false negatives (FNs) in our dataset, and performance for each class was then calculated based on precision (P = TP/(TP+FP)), recall (R = TP/(TP+FN)), and F-score, which is the first harmonic mean of precision and recall (F-score = 2×P×R/(P+R)).

2.2.4. Image post-processing and concentration estimates

Final vignettes were merged with simultaneously collected environmental data using the time stamp and binned into 1 m vertical depths along the ISIIS towpath. Fluorescence volts were converted to chl *a* concentrations based on a calibration for our instrument done by SeaBird on 29 January 2016, and environmental data were kriged (Matlab package 'EasyKrig' v.3.0) onto a grid equal to the length of each transect at 1 m vertical and 500 m horizontal resolution. Plume waters were defined using the reference salinity of ≤32.5 for the CRP (Barnes et al. 1972).

Taxa concentrations (ind. m^{-3}) were estimated using the volume of water imaged, average tow speed, and time spent in each 1 m bin. A correction factor based on the confusion matrix results (Hu & Davis 2006, Schmid et al. 2020) was applied to the calculated concentrations according to the following equation

$$\text{Correction factor}_{\text{taxon}} = \frac{\text{Precision rate}_{\text{taxon}}}{\text{Recall rate}_{\text{taxon}}} \quad (1)$$

2.3. Ecological analyses

Key taxonomic groups were selected for analysis based on their ecological significance as potential prey or predator groups of larval fishes. Calanoid copepods and appendicularians are frequently found in the guts of larval fishes (Baier & Purcell 1997, reviewed by Llopiz 2013). Appendicularians, in particular, are estimated to comprise 97% of the diet of a pleuronectid in this region (Gadomski & Boehlert 1984). Calanoid copepods dominate the plankton off Oregon (Peterson & Miller 1975) and are a more important prey resource than cyclopoid copepods at mid- and high latitudes (Llopiz 2013). Chaetognaths are primarily carnivorous, and several studies suggest that based on their high abundance and the presence of fish larvae in their guts, they may cause significant mortality (reviewed by Alvarino 1985). Finally, larval

fishes make up a significant portion of the diets of some gelatinous taxa, including ctenophores, siphonophores, and hydromedusae (reviewed by Purcell 1985). With few notable exceptions (Gadomski & Boehlert 1984), there is a lack of information on the diets of and predation upon larval fishes in the NCC compared to other regions (e.g. the Straits of Florida; see Llopiz & Cowen 2009). To account for this knowledge gap, zooplankton were combined into the following higher taxonomic groupings for all analyses: larval fishes, calanoid copepods, appendicularians, chaetognaths, ctenophores, hydromedusae, and siphonophores. Concentrations of each taxon per depth bin along the sampling transects were calculated, and Kruskal-Wallis tests were used to compare the mean concentrations in plume (salinity ≤32.5) and non-plume waters (salinity >32.5). Finally, each individual within these taxa was measured along its major axis. Taxa size distribution plots were created to evaluate the potential for predator–prey interactions.

2.3.1. Zooplankton community analyses

Ordination was used to determine if the zooplankton community structure differed between the 2 plume types (tidal plume and far-field plume) and oceanic habitat. Data were binned into 1 m vertical depth bins across each transect. Tidal plume habitats were defined as those directly off of the river mouth (Transects 1 and 2) where salinity was ≤32.5, far-field plume habitats were classified by the same salinity value but located inshore, south of the river mouth (Transect 3 inshore), and oceanic habitats were where salinity was >32.5.

Ordination was done using non-metric multidimensional scaling (NMDS) in the R (v. 3.5.2) package 'vegan' v. 2.5-6 (Oksanen et al. 2019) with a Bray-Curtis distance measure. NMDS ordinates sample units (1 m depth bins across each transect) in multidimensional species space to identify samples with similar zooplankton communities, where the more similar in composition 2 samples are, the closer they appear in space. The relationship between stress and dimensionality was examined to find the smallest number of axes where the reduction in stress (a measure of the goodness-of-fit between the species data and the final ordination) adequately plateaued (Mather 1976). The 2 dominant ordination axes are presented graphically for ease of visualization. We tested the null hypothesis of no difference in zooplankton communities among tidal plume, far-field plume, and oceanic habitats using the 'adonis' function in 'vegan,' which computes a non-parametric permutational multivariate analysis of variance (Anderson 2001).

2.3.2. Fine-scale vertical distributions

Mean concentrations per 1 m depth bin of larval fishes, their prey, and their predators were examined to investigate the effect of plume waters on taxa vertical distributions. The weighted mean depth (WMD) of the vertical distribution of larval fishes and their potential prey and predators was calculated following Frost & Bollens (1992):

$$\mathrm{WMD} = \frac{\sum (n_i \times d_i)}{\sum n_i} \tag{2}$$

where n_i is the concentration of individuals per cubic meter of taxon i at depth d_i, which is taken to be the shallowest point of each 1 m depth stratum. WMDs were calculated for the full transects as well as the deeper southern and shallower northern portions of the cross-plume transects separately to ensure that patterns were not significantly influenced by the bathymetry of the region.

2.3.3. Larval fish prey/predator spatial overlap

Relationships of larval fish prey/predator taxa throughout the water column were evaluated using the spatial overlap index described by Williamson & Stoeckel (1990):

$$O_{ij} = \frac{\sum_{z=1}^{m} \left(N_{jz} \times n_{iz}\right) m}{\sum_{z=1}^{m} \left(N_{jz}\right) \times \sum_{z=1}^{m} \left(n_{iz}\right)} \tag{3}$$

where z is the depth stratum, m is the number of sampled depths, N_{jz} is the concentration of larval fish at a given depth, and n_{iz} is the concentration of the select prey or predator taxon at a given depth. Overlap index values of 1 indicate that fish larvae and/or the select taxonomic group are evenly distributed in the water column; index values <1 indicate vertical spatial separation between fish larvae and the select taxa; and index values >1 indicate vertical spatial overlap of fish larvae and the select taxa, where the theoretical upper limit is defined by the number of points sampled. The spatial overlap index of Williamson & Stoeckel (1990) takes into account prey and predator concentrations in addition to spatial and temporal overlap and has been used in a variety of systems to evaluate trophic interactions among zooplanktonic organisms (Bezerra-Neto & Pinto-Coelho

2007, Möller et al. 2012, Picapedra et al. 2015). Overlap indices for larval fishes and each of their prey/predator groups were determined for every quasi-vertical profile (2 per undulation) resulting in horizontally stratified index values. Median transect-wide integrated values with their corresponding standard errors were calculated based on the individual quasi-vertical profile spatial overlap values and are also reported to provide an overall statistical description of overlap in each transect.

2.3.4. Overlap-environment modeling

Boosted regression tree (BRT) analysis was used to evaluate how the presence of surface plume waters affected the likelihood of spatial overlap between larval fishes and their prey/predator taxa in the water column. BRTs are an ensemble statistical modeling method capable of fitting complex nonlinear relationships (Luo et al. 2014, Lieske et al. 2018). Instead of attempting to fit a single parsimonious model like traditional techniques, BRTs use random subsets of data to construct a large number of simple regression trees. These trees are then combined using machine learning (boosting) to optimize predictive performance (Elith et al. 2008). Similar to other tree-based methods, BRTs provide an estimate of the relative importance of each explanatory variable as well as partial dependence plots that show how the influence of the variable varies over its range.

Six BRT models (one for each prey/predator taxon) were constructed to predict the horizontally stratified spatial overlap index based on 5 explanatory variables: mean salinity, temperature, dissolved oxygen, chl *a* concentration, and photosynthetically active radiation (E_{PAR}) in surface waters. Specifically, each row in the model matrix consisted of the calculated spatial overlap index for one quasi-vertical profile and the mean environmental parameters in the top 5 m of the water column for that profile. We used the top 5 m to indicate surface waters because plumes are shallow features; during sampling, the maximum depth of the plume was 3.7 m in some regions, and the plume signal was quickly lost beyond this depth during the ebb tide due to sharp physical gradients. All models were built using the R (v.3.5.2) package 'dismo' v.1.1-4 (Hijmans et al. 2017), and model performances were evaluated using an estimate of deviance explained (D^2 = 1 – residual deviance/null deviance). Partial dependence plots were created for the top 3 most important explanatory variables for each prey/predator taxon using the R (v.3.5.2) package 'gbm' v.2.1.5 (Greenwell et al. 2019). Partial dependence plots show the effect of environmental variables on the likelihood of spatial overlap between larval fish and each prey/predator group.

3. RESULTS

3.1. Environmental setting

Mean Columbia River discharge during the study period was 5478 m^3 s^{-1}, with a maximum flow volume of 11 100 m^3 s^{-1}. Winds reversed from weakly downwelling-favorable to upwelling-favorable 8 d prior to sampling and remained weakly upwelling-favorable throughout the sampling period (Fig. 1B). The sampling period encompassed spring tides; the semidiurnal tides were unequal in magnitude, with the larger ebb occurring during daytime hours and coinciding with sampling (Fig. 1C). Transect 1 data were primarily collected during slack ebb and Transect 2 during slack flood. Transect 3 (cross-shelf) sampling began just before slack ebb and continued through maximum flood, when sampling was nearest to shore. Plume waters (defined as salinity ≤32.5) were present at the surface and captured in sampling during all transects.

3.2. Automated classification performance

Imagery data yielded 24.7 million vignettes, including numerous representatives of all taxa of interest (6095 fish larvae and ~1.5 million prey/predator zooplankton; Fig. 2). After filtering thresholds were applied and the original 161 classes were mapped onto their broader groups, the weighted average model precision (number of true positives/number of true and false positives) was 77%, recall (number of true positives/number of true positives and false negatives) was 73%, and F-score (harmonic mean of precision and recall) was 67%. Note that a correction factor (precision/recall, see Section 2.2.4) was applied prior to calculating final concentrations (Table S2, Fig. S1). These evaluation metrics are strong, especially given the large number of classes included in our training library (n = 161). As the number of classes in a model increases, classification becomes more difficult. Yet, our model precision is comparable to studies with far fewer classes. For example, Gorsky et al. (2010) achieved a mean model precision of ~80% (precision calculated as recall/[recall + contamination] in their study) with just 8 classes, while our mean model precision of 77% was achieved with 161 classes. Our

Table 1. Mean (SE) taxa concentrations per depth bin along the sampling transect for all sampling (total) and each sampling transect near the Columbia River Plume including the significance of a Kruskal-Wallis (K-W) test for differences in mean concentrations in the plume (P) vs. outside of the plume (NP). Taxa are in descending order based on their concentrations within each sampling regime. K-W test significance: *p < 0.001, **p < 0.0001, (–): not significant. Sample sizes for concentration (n1) and K-W estimates (n2) are indicated under each transect. NA: no K-W test was performed due to a lack of plume waters

Transect	Taxon	Mean concentration (ind. m^{-3})	SE	K-W (P/NP)
Total	Appendicularians	81.14	1.26	**
n1 = 7504	Calanoid copepods	15.05	0.22	**
n2 (P/NP) = 2459/5045	Hydromedusae	9.06	0.24	**
	Chaetognaths	7.04	0.12	**
	Ctenophores	2.01	0.04	**
	Siphonophores	1.97	0.03	**
	Fish larvae	0.11	0.00	**
Transect 1 (Ebb)	Appendicularians	50.04	1.09	**
n1 = 1835	Calanoid copepods	14.06	0.40	**
n2 (P/NP) = 575/1260	Hydromedusae	11.79	0.45	**
	Chaetognaths	9.30	0.27	**
	Ctenophores	2.41	0.08	**
	Siphonophores	2.11	0.07	**
	Fish larvae	0.09	0.00	**
Transect 2 (Flood)	Appendicularians	50.04	1.15	**
n1 = 2337	Hydromedusae	13.43	0.62	**
n2 (P/NP) = 838/1499	Calanoid copepods	11.85	0.33	**
	Chaetognaths	11.45	0.27	**
	Ctenophores	2.51	0.08	**
	Siphonophores	2.32	0.06	**
	Fish larvae	0.12	0.01	**
Transect 3 (inshore)	Appendicularians	219.56	5.24	**
n1 = 1211	Calanoid copepods	33.86	0.78	**
n2 (P/NP) = 213/998	Hydromedusae	7.64	0.49	–
	Chaetognaths	5.01	0.15	**
	Siphonophores	2.41	0.09	*
	Ctenophores	2.37	0.08	**
	Fish larvae	0.16	0.01	**
Transect 3 (offshore)	Appendicularians	61.26	1.25	NA
n1 = 2121	Calanoid copepods	8.25	0.20	NA
	Hydromedusae	2.59	0.10	NA
	Chaetognaths	1.34	0.04	NA
	Siphonophores	1.18	0.04	NA
	Ctenophores	0.86	0.03	NA
	Fish larvae	0.10	0.01	NA

model also performed well compared to more recent studies that use CNNs. Orenstein et al. (2015) presented a comparison of different classifiers, of which the best one had 70 classes, and had an unweighted mean F-score of 42%.

3.3. Taxa concentrations

A total of 6095 fish larvae were identified in the automated image classification. The most abundant groups accounted for 83.86% of the catch and were comprised of Sebastidae (43.58%), Clupeiformes (19.76%), 'long slender' (10.19%), Pleuronectiformes (8.33%), and Myctophidae (2.00%). Based on the literature in this region, we suspect that the group 'long slender' was possibly dominated by Bathylagidae (Parnel et al. 2008). Mean concentrations of taxa of interest during all sampling varied over 3 orders of magnitude (Table 1). Corrected larval fish concentrations ranged from 0.09 ± 0.00 ind. m^{-3} in Transect 1, to 0.16 ± 0.01 ind. m^{-3} in the inshore region of Transect 3. Appendicularians were the most abundant overall (81.14 ± 1.26 ind. m^{-3}) followed by calanoid copepods (15.05 ± 0.22 ind. m^{-3}). Calanoid copepods and appendicularians were also most abundant in all individual transects with the exception of Transect 2, where the concentration of hydromedusae (13.43 ± 0.62 ind. m^{-3}) exceeded that of calanoid copepods (11.85 ± 0.33 ind. m^{-3}). Predator groups were dominated by hydromedusae and chaetognaths, with total mean concentrations of 9.06 ± 0.24 and 7.04 ± 0.12 ind. m^{-3}, respectively. The offshore region of Transect 3 had the lowest abundances of copepods (8.25 ± 0.20 ind. m^{-3}), chaetognaths (1.34 ± 0.04 ind. m^{-3}), ctenophores (0.86 ± 0.03 ind. m^{-3}), hydromedusae (2.59 ± 0.10 ind. m^{-3}), and siphonophores (1.18 ± 0.04 ind. m^{-3}), and the second lowest concentration of fish larvae (0.10 ± 0.01 ind. m^{-3}).

Concentrations of all taxa differed significantly between the plume and non-plume water masses in regions where the plume was present, with the exception of hydromedusae in the inshore region of Transect 3 (Kruskal-Wallis test; Table 1). In all other cases, taxa concentrations were significantly higher in non-plume water compared to plume water.

3.4. Taxa size distributions

The size (total length; TL) of larval fishes ranged from 1.00 to 38.75 mm, with a mean TL of 6.44 mm (Table 2). Fishes south of the river mouth were larger than those directly off of the river mouth. The size of prey and predator taxa also varied across transects, but both prey groups (calanoid copepods and appen-

Table 2. Mean taxa size (mm) and standard error for each sampling transect near the Columbia River Plume

Taxon	Transect 1 (ebb)		Transect 2 (flood)		Transect 3 (inshore)		Transect 3 (offshore)	
	Mean	SE	Mean	SE	Mean	SE	Mean	SE
Fish larvae	5.70	0.09	5.54	0.08	7.88	0.12	6.63	0.09
Calanoid copepods	2.72	0.01	2.77	0.01	3.64	0.01	2.22	0.01
Appendicularians	2.80	0.00	2.80	0.00	2.77	0.00	2.73	0.00
Chaetognaths	6.59	0.01	7.03	0.02	8.36	0.03	8.29	0.04
Ctenophores	4.51	0.03	4.18	0.03	4.50	0.04	8.62	0.11
Hydromedusae	14.67	0.05	15.28	0.05	12.18	0.08	5.31	0.05
Siphonophores	9.42	0.03	9.08	0.04	6.93	0.06	6.16	0.07

dicularians) were substantially smaller than larval fishes in all sampling. Mean larval fish TL ranged from 2.74 to 5.11 mm larger than the mean size of their prey. In general, potential predator size distributions were more protracted and their distributions overlapped with, and often exceeded, those of larval fishes (Fig. S2). The exceptions to this were ctenophores, whose size distributions were more compressed and had a mean size that was smaller than those of larval fishes in all plume regions. Conversely, the mean size of hydromedusae exceeded that of larval fishes in all plume regions (i.e. in all sampling but the offshore region of Transect 3). While chaetognaths were on average larger than larval fishes throughout the entirety of sampling, siphonophores were larger than larval fishes only directly off of the river mouth (Table 2).

3.5. Plume structure, community composition, and fine-scale vertical distributions

The distribution of larval fishes, their prey, and their predators in relation to the CRP was documented for 4 distinct water column structures observed throughout sampling.

3.5.1. Transect 1: ebb tidal plume — low surface salinity and strong shallow stratification

Low-salinity plume waters were present at the sea surface along the entire length of Transect 1. The plume was highly stratified and restricted to the upper 20 m of the water column with vertical salinity gradients of up to 4.4 m^{-1} and a maximum depth of 19.6 m. Minimum depth of the plume was 4.5 m (Fig. 3A).

With the exception of a small pocket of fresher water extending to 19.6 m depth on the southern end of the transect, the plume was deeper in the northern than the southern extremes of the transect. Salinity values ranged from 12.68 at the surface to 34.39 at depth. The freshest water was located directly offshore of the river mouth, in the upper 3 m of the water column. Surface salinity was higher in the southern portion of the transect, with a minimum salinity of 25.23 in the upper 20 m. Temperature varied from 7.55 to 15.0°C, with the warmest waters in the top 15 m on the northern end of the transect. A thin phytoplankton layer (as indicated by chl *a* concentration) extended approximately 6 km into the southern portion of the transect. The entire water column was normoxic, with oxygen values exceeding 1.43 ml l^{-1} (Fig. 3A; Grantham et al. 2004).

During the ebb tide when there was strong, but shallow, stratification of the water column, larval fishes did not occupy the shallowest 5 m, but were relatively evenly distributed below this depth with a slight peak in abundance ~10 m below the base of the plume (Fig. 4A). While prey groups (calanoid copepods and appendicularians) were broadly distributed below 5 m depth, their WMDs were slightly deeper than that of larval fishes, with the exception of appendicularians in the southern region. Predator distributions were more dynamic but were generally most abundant in the top 25 m of the water column. The WMD of predators was, on average, 7.85 m shallower than the WMD of fish larvae in the southern region and 1.30 m shallower in the northern region. Chaetognath and hydromedusae distributions formed distinct concentration peaks near the base of the plume, while the distributions of ctenophores and siphonophores were more protracted. Notably, chaetognaths were the only taxon present in significant concentrations at the shallowest depths and some of the lowest salinities in this transect (~15; Fig. 4A; Fig. S3A).

3.5.2. Transect 2: flood tidal plume — moderately low surface salinity and stratification

Plume waters remained at the sea surface along the entirety of Transect 2. While still highly stratified, the plume was more mixed during the flood than the ebb tide, with a maximum vertical salinity gradient of 2.1 m^{-1} and salinity values ranging from 17.94 within the surface plume to 35.02 at

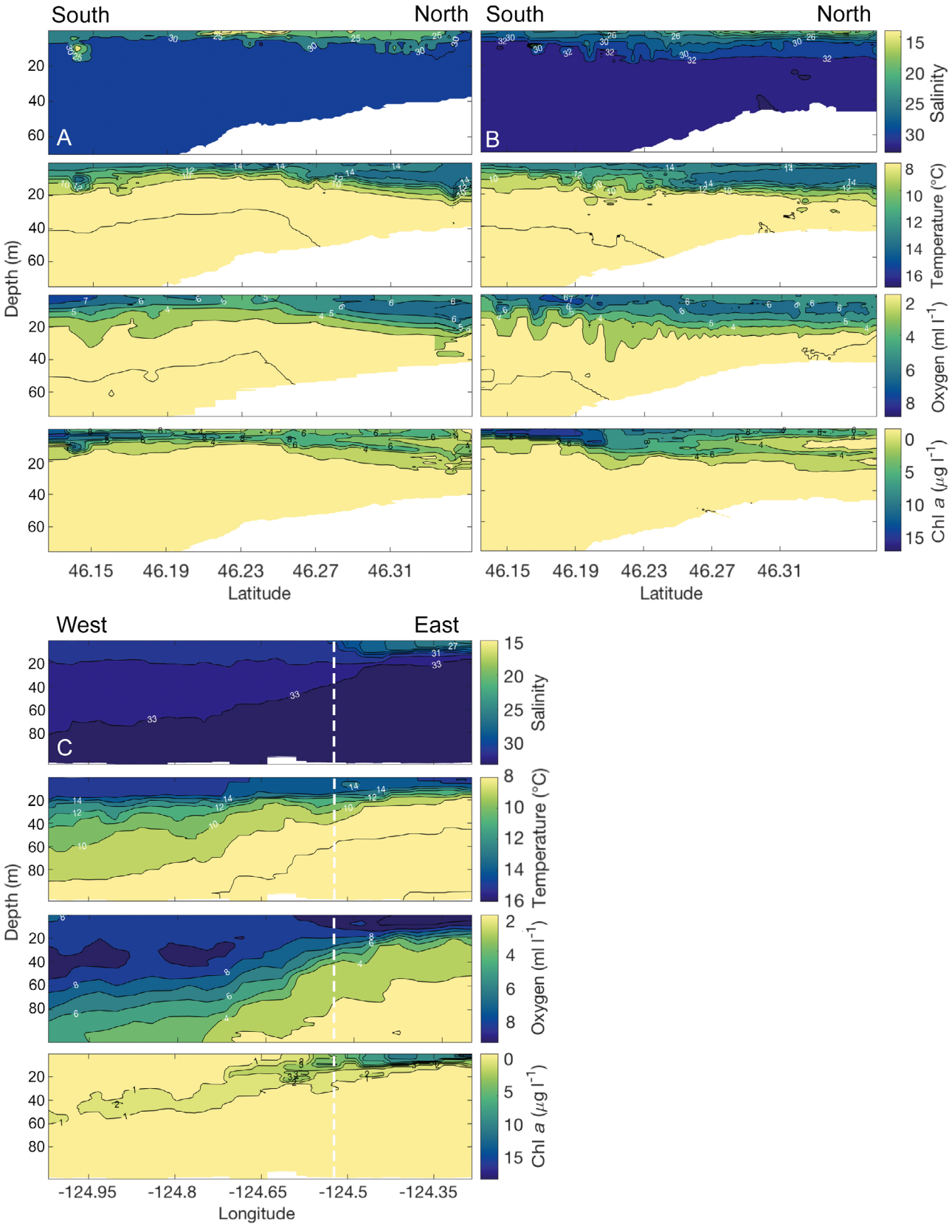

Fig. 3. Kriged contour plots of environmental parameters during (A) Transect 1 (ebb), (B) Transect 2 (flood), and (C) Transect 3 near and within the Columbia River Plume. The dashed line in C indicates the cutoff between the inshore and offshore regions used in analyses. Chl *a*: chlorophyll *a* concentration

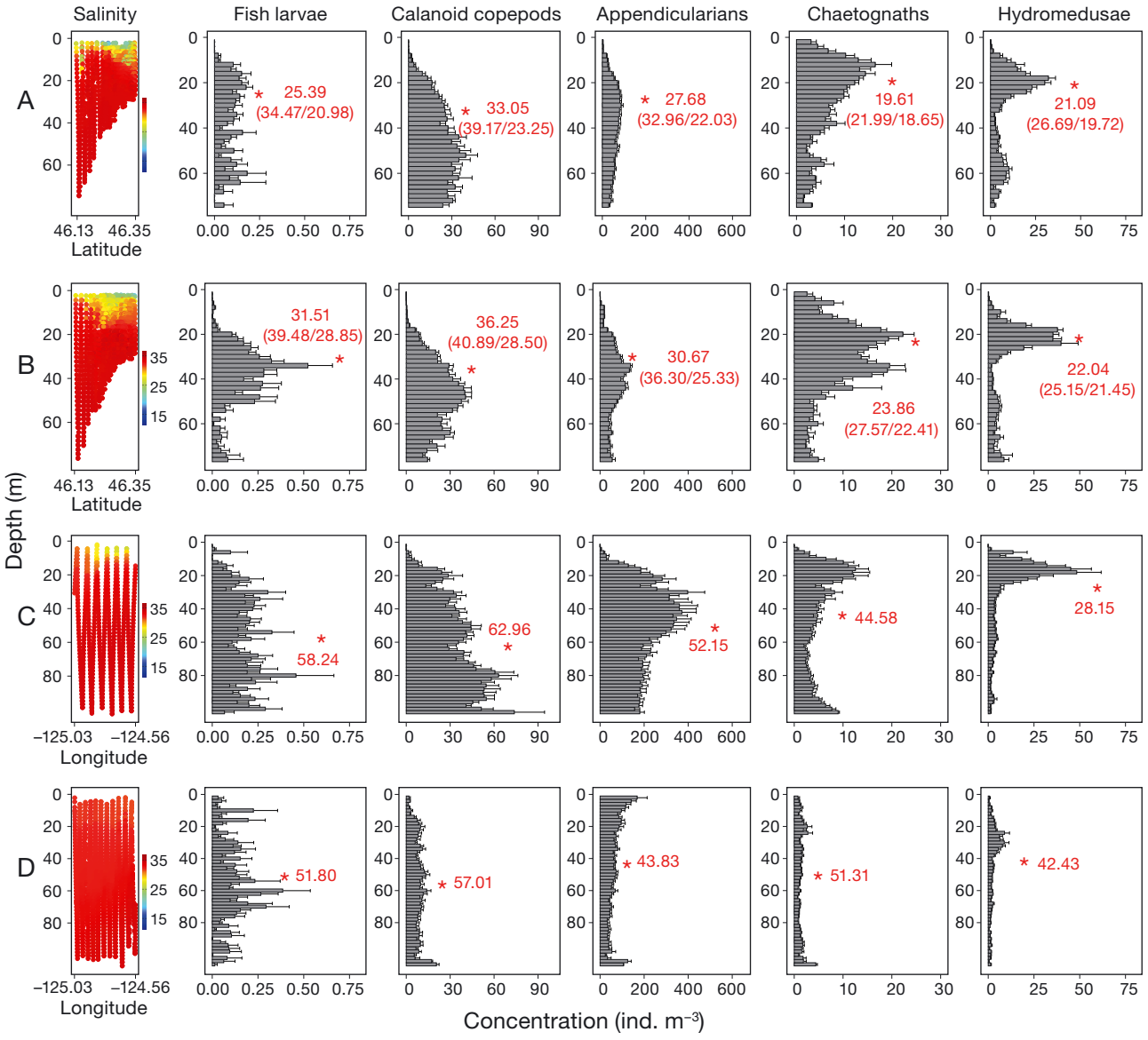

Fig. 4. Mean concentration of each taxonomic group in every other 1 m depth bin during (A) Transect 1, (B) Transect 2, (C) Transect 3 inshore, and (D) Transect 3 offshore of the Columbia River, with transect salinity profiles shown in the far left column. Error bars are standard error, and red asterisks indicate the weighted mean depth (WMD; in meters) of taxa distributions. For transects (A) and (B), we also give separate WMDs for the southern (deep) and northern (shallow) sections of the transect separately as (south/north)

depth. Again, the plume was restricted to the top 20 m of the water column varying in depth from 3.7 m in the south to 17.6 m in the north. While the temperature range during the flood tide was similar to the ebb (7.58–14.93°C), the extent of the 'warm pool' of water in the northern portion of the transect surface waters increased both vertically and horizontally. Similarly, the phytoplankton layer on the southern end of the transect became more well-defined and increased in thickness from around 5 to 10 m depth. Oxygen values ranged from 1.67 to 7.62 ml l^{-1} (Fig. 3B).

There was a distinct deepening (>6 m) of the vertical distribution of larval fishes from a WMD of 25.39 m during the ebb tide to 31.51 m during the flood tide when low-salinity water extended deeper into the water column (Figs. 3B & 4B). This pattern held in the deep and shallow portions of the transect where the WMD of larval fishes deepened 5.01 m in the south and 7.87 m in the north. Larval fish concentrations were negligible above 20 m depth, and there was a broad peak in abundance at the 20–50 m depth range, indicating possible vertical compression. WMDs of calanoid copepod and appendicularian prey

deepened by approximately 3 m, creating moderate abundance peaks at depth that roughly coincided with the peak in larval fish abundance. When the transect was split into deep and shallow sections, the WMD of fish larvae closely adhered to both prey groups, especially calanoid copepods. One predator taxon, ctenophores, exhibited a vertical distribution markedly similar to larval fishes. Chaetognath, hydromedusae, and siphonophore WMDs were, at a minimum, 6.44 m shallower than the WMD of fish in the northern region and 8.94 m shallower in the southern region. Interestingly, the distribution of hydromedusae was virtually the same in the ebb and flood stages of sampling, with a strong peak in concentration around 20 m depth. Although there remained some degree of overlap with the vertical distribution of fish larvae, the highest peak in larval fish abundance was nearly 10 m deeper than the region of highest hydromedusae concentrations (Fig. 4B; Fig. S3B).

3.5.3. Transect 3 (inshore): far-field plume — intermediate surface salinity and weak stratification

Low-salinity waters extended 18 km into Transect 3 (cross-shelf, south of the river mouth) on the inshore end (Fig. 3C). Salinity values within the plume reached a minimum of 25.1, and the maximum depth of the plume was 15.5 m. The maximum vertical salinity gradient was 0.5 m^{-1}. Temperature was moderately cooler in this region south of the river mouth and ranged from 6.97 to 15.19°C. The highest phytoplankton signal was located closest to shore, with a maximum chl *a* concentration of 10.39 µg l^{-1} . Bottom water beneath the plume was mildly hypoxic, reaching a minimum of 1.36 ml l^{-1}.

High abundances of larval fishes were relatively evenly distributed throughout the water column. WMD of fish larvae was deepest in this region at 58.24 m (Fig. 4C). The same was true for calanoid copepods (62.96 m) and appendicularians (52.15 m), yet their distributions appeared to be more structured. Calanoid copepod abundance increased slightly with depth, and appendicularians peaked in the 20–60 m depth range. The 1 m depth bin with the highest concentration of fish larvae coincided with a 6 m peak in copepod abundance. WMD of fish larvae was <1.5 m deeper than the mean for prey, but was nearly 8 m deeper than the mean for predators. Again, hydromedusae exhibited the most contracted distribution of any taxon, displaying a sharp, shallow concentration peak. Their WMD was >30 m shallower than the WMD of fish larvae (Fig. 4C; Fig. S3C).

3.5.4. Transect 3 (offshore): negligible plume

In the cross-shelf offshore region, salinity ranged from 31.58 to 33.92. Despite the relatively minor salinity variability, the water column was moderately structured by thermo- and oxyclines shoaling toward the shelf, with values ranging from 7.11 to 15.75°C and 1.53 to 6.70 ml l^{-1}, respectively (Fig. 3C). The maximum phytoplankton chl *a* concentration of 4.63 µg l^{-1} was substantially lower than in all other regions. In the absence of surface plume waters, larval fishes and all zooplankton were relatively evenly distributed in the water column (Fig. 4D; Fig. S3D).

3.5.5. Community composition

Non-metric multidimensional scaling (NMDS) revealed significant differences in the community compositions among the 2 types of plume habitats (tidal and far-field plume) and oceanic waters (Fig. 5). The ordination performed well with a stress value of 0.08, which is in the 'good' criteria range (McCune & Grace

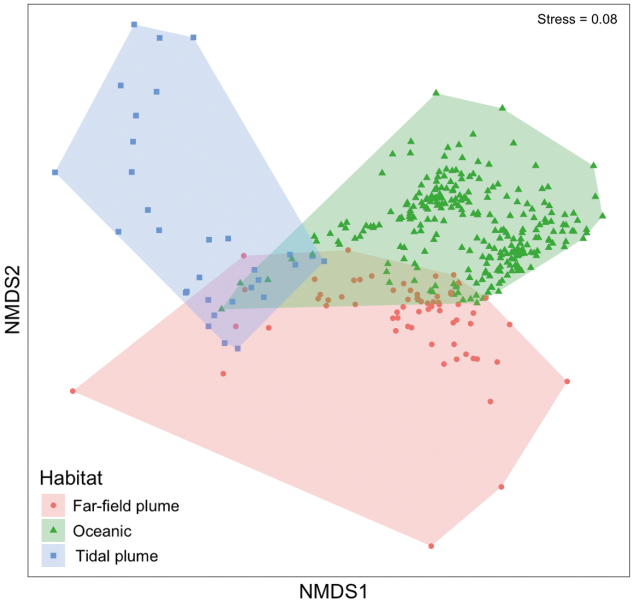

Fig. 5. Non-metric multidimensional scaling (NMDS) ordination of zooplankton taxa concentrations in 3 different habitats near the Columbia River Plume. Each data point represents the community composition in a 1 m vertical depth bin along the sampling transects. Tidal plume samples are those within plume waters directly off of the river mouth, far-field plume samples are plume waters south of the river mouth, and oceanic samples are those with salinity >32.5. Stress (a measure of goodness-of-fit) is indicated in the top right corner

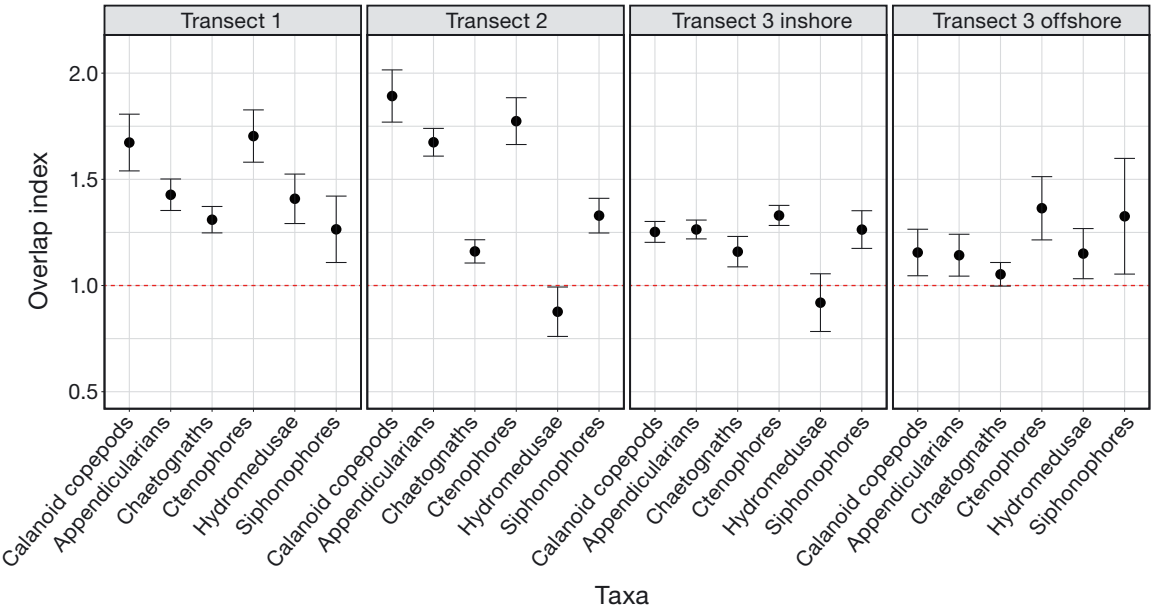

Fig. 6. Median spatial overlap of selected prey and predator groups with fish larvae in transects near and within the Columbia River Plume. Black markers are estimates of the Williamson spatial overlap index during each sampling transect. Overlap index values = 1 (red dashed line) indicate that fish larvae and the taxonomic group are evenly distributed in the water column; index values <1 indicate some degree of vertical separation between fish larvae and the group; index values >1 indicate some degree of vertical overlap of fish larvae and the group in any layer of the water column. Error bars are standard error

2002). Non-parametric statistical analysis ('adonis') indicated that the zooplankton community structure was significantly different among the tidal plume, far-field plume, and oceanic habitats (p = 0.001).

3.6. Larval fish prey/predator spatial overlap

As an indication of the potential for trophic interactions between larval fishes and their prey/predators, we calculated an index of vertical overlap for each sampling quasi-vertical profile (n = 152) along every transect. Median transect-wide overlap indices ranged from 1.14 to 1.89 for prey groups and from 0.88 to 1.77 for predator groups (Fig. 6). Taxa spatial overlap with larval fishes varied significantly over space (Transect 3: inshore vs. offshore) and time (Transect 1: ebb tide vs. Transect 2: flood tide; Figs. 6 & 7).

3.6.1. Variation in overlap over space

When no plume waters were present, there was some degree of spatial overlap between larval fishes and all prey and predator taxa (Fig. 6). Overlap between prey/predator taxa and fish larvae was more dynamic in regions where the water column was structured by the inshore plume, as evident by the overlap of larval fishes with some taxa and the separation from others. Where plume waters were present at the surface, south of the river mouth (i.e. Transect 3 inshore), there was a small degree of vertical alignment between fish larvae and calanoid copepods, appendicularians, chaetognaths, ctenophores, and siphonophores, while there was vertical separation between fish larvae and hydromedusae (Fig. 6).

Across Transect 3, prey groups overlapped with fish larvae throughout the entire length of the inshore region, but there were instances of separation from fish larvae in the offshore region. With the exception of chaetognaths, all taxa anomalously overlapped with fish larvae in one quasi-vertical profile offshore (Fig. 7C,D).

Interestingly, along the leading edge of the plume (i.e. the vertical plume front; second to farthest west quasi-vertical profile in Fig. 7C), spatial overlap of prey taxa with larval fishes was nearly 2 standard deviations above the mean of adjacent waters. There was an even greater increase (2.5 standard deviations above the mean) in spatial overlap with predator taxa near the vertical plume front. A few kilometers offshore of this frontal region, prey groups only slightly co-occurred with or were separated from fish larvae, while predator groups highly co-occurred with fish larvae (Figs. 7C, D).

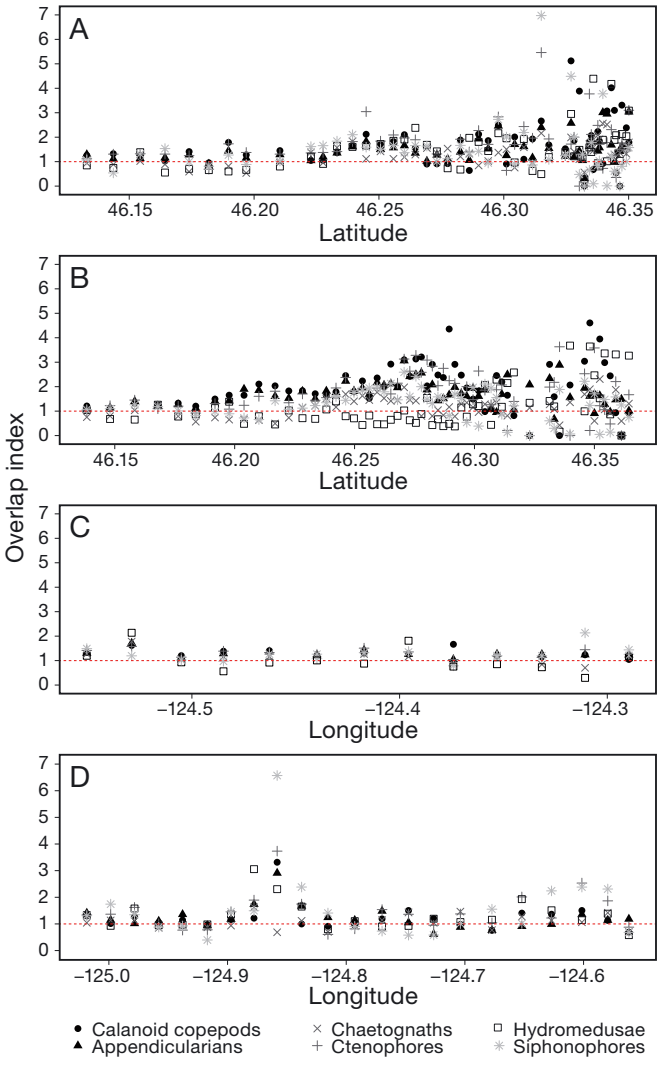

Fig. 7. Spatial overlap between fish larvae and selected prey and predator groups along (A) Transect 1, (B) Transect 2, (C) Transect 3 inshore, and (D) Transect 3 offshore near and within the Columbia River Plume. Markers are estimates of the Williamson spatial overlap index for each quasi-vertical profile; details as in Fig. 6

3.6.2. Variation in overlap over time

Median overlap values indicated that all prey and predator taxa were positively correlated with fish larvae during the ebb tide (Transect 1; Fig. 6). During the flood tide (Transect 2) a few hours later, while both prey taxa (calanoid copepods and appendicularians) became more strongly correlated with fish larvae, 3 out of 4 predator groups became less correlated with fish larvae (chaetognaths and siphonophores) or even showed some degree of vertical separation (hydromedusae; Fig. 6).

Notably, where plume waters were the freshest and very shallow during the ebb tide, all taxa were correlated with fish larvae (Figs. 3A & 7A). This contrasts with both north and south of this region where there was a mixture of overlap and separation across taxa (Fig. 7A). When the river was flooding and low-salinity water was pushed deeper into the water column (Fig. 3B), there was a high overlap of larval fishes with both prey groups (calanoid copepods and appendicularians) but separation between fish larvae and some predator taxa, especially hydromedusae (Fig. 7B).

Spatial overlap of taxa with larval fishes was more accentuated in the shallower northern portion of Transects 1 and 2. Generally, in the deeper portion of the transect to the south, prey groups overlapped with fish larvae and predator groups were separated from fish larvae (Fig. 7A,B).

3.7. Overlap-environment modeling

The number of regression trees fit to BRT models ranged from 1100 for the overlap model of larval fishes with appendicularians, to 3000 for the overlap model of larval fishes with ctenophores. All models performed well, with a mean D^2 of 0.48. Ctenophore and hydromedusae models performed best, with D^2 values of 0.65 and 0.62, respectively (Fig. 8).

Model results indicate that salinity and chl *a* concentration had the highest relative influence on spatial overlap with larval fishes for the largest number of taxa. Salinity was the most important variable influencing overlap for 3 taxa and was in the top 3 most important for all taxa (Fig. 8). The next most influential explanatory variables, based on rank importance, in decreasing order, were chl *a* concentration, temperature/oxygen, and E_{PAR}.

The mean relative influence of salinity on spatial overlap with larval fishes was greater for prey groups (33.95%) compared to predator groups (24.08%; Fig. 8). Chaetognath overlap with fish larvae was the least influenced by salinity (18.7%), and they were the only group to not have salinity in the top 2 most important variables (Fig. 8).

Partial dependence plots showing the effect of environmental variables on the spatial overlap index relative to the model mean indicated that all taxa were predicted to have above-average spatial overlap with larval fishes when surface salinity was ≤24 (Fig. 9). Maximum overlap of larval fishes with copepods occurred when surface salinity was ~24, while overlap with appendicularians was greatest when surface salinities were ~25.5–27. Chaetognath overlap

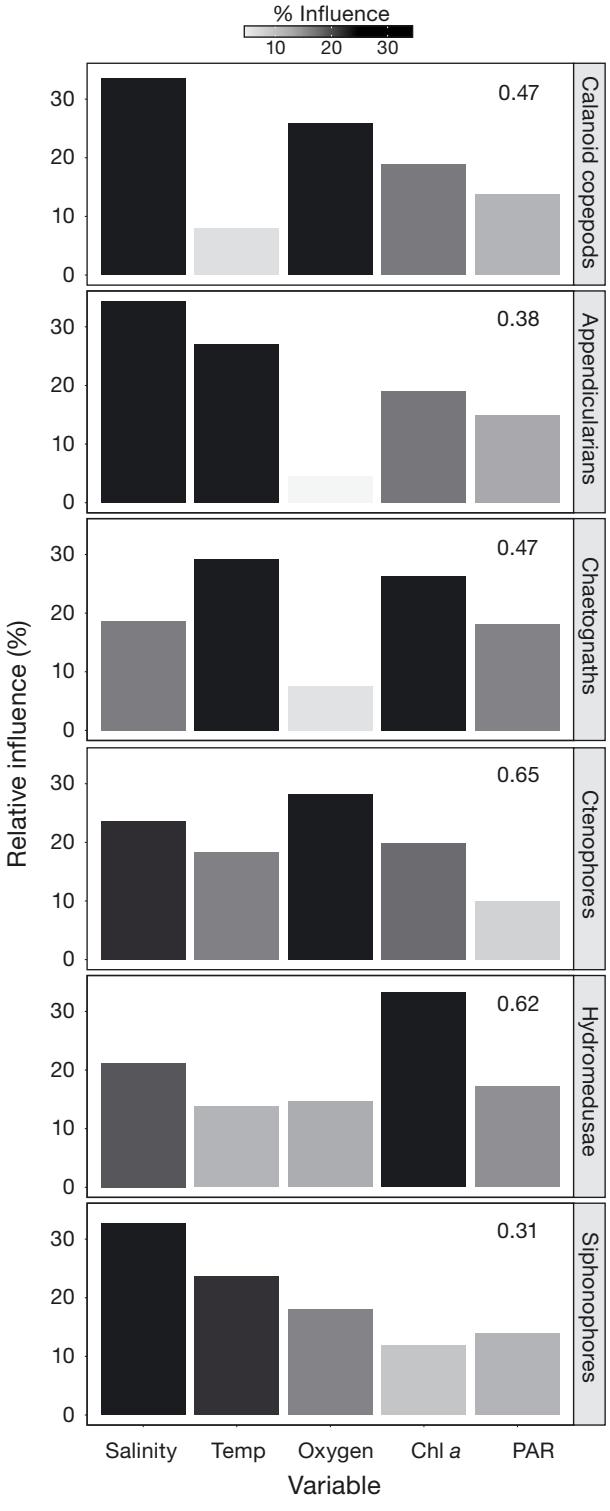

Fig. 8. Results of the boosted regression tree (BRT) analysis showing the relative influence of surface physical variables on the spatial overlap of each taxon with fish larvae near and within the Columbia River Plume. Associated model deviance explained (D^2) values are in the top right corner of each plot. Chl *a*: chlorophyll *a* concentration; PAR: photosynthetically active radiation

with larval fishes was at a maximum at ~26.5, ctenophores and siphonophores at ~20–24, and hydromedusae at ~24.5–26. When surface salinity approached the reference plume cut off for the CRP (≤32.5), all taxa were predicted to have below-average overlap with larval fishes (Fig. 9).

Copepods and appendicularians showed above-average spatial overlap with larval fishes at high surface chl *a* concentrations, while chaetognaths, ctenophores, and hydromedusae demonstrated below-average overlap at these values (Fig. 9). In general, intermediate surface temperatures (~13–15°C), high surface oxygen (~6 ml l^{-1}), and the highest surface E_{PAR} values (>0.002) predicted above-average spatial overlap with larval fishes (Fig. 9).

4. DISCUSSION

Using a high-resolution *in situ* imaging system, we documented changes in the fine-scale horizontal (km) and vertical (m) distributions and spatial overlap of larval fishes with their zooplankton prey and predators in a highly dynamic river plume system. Our analyses demonstrated substantial changes in concentrations, distributions, and spatial overlap with larval fishes among different zooplankton taxa over small spatial and temporal scales.

Our results are consistent with previous findings that suggested chl *a*, zoo-, and ichthyoplankton concentrations are higher in plume-influenced regions (St. John et al. 1992, Albaina & Irigoien 2004, Morgan et al. 2005), yet emphasize that zoo- and ichthyoplankton were primarily found aggregated beneath, and not within, the plume at the horizontal plume front. Fish larvae and their prey (calanoid copepods and appendicularians) were generally distributed deeper in the water column than their potential predators (chaetognaths, ctenophores, hydromedusae, and siphonophores). However, the presence of a shallow horizontal plume front reduced the magnitude of this difference, contributing to high spatial overlap of larval fishes with their prey and predators (although overlap with predators was taxon-specific and varied with the tide and depth of the horizontal front). Further, regions of high taxa concentration did not necessarily lead to high fine-scale spatial overlap of larval fishes with their prey/predators. Surface salinity and chl *a* concentration were the most important factors influencing spatial overlap of larval fishes and zooplankton taxa.

Larval fishes must find food and avoid predators in heterogeneous environments (Lasker 1975, Bailey & Houde 1989, Cushing 1990). In highly dynamic sys-

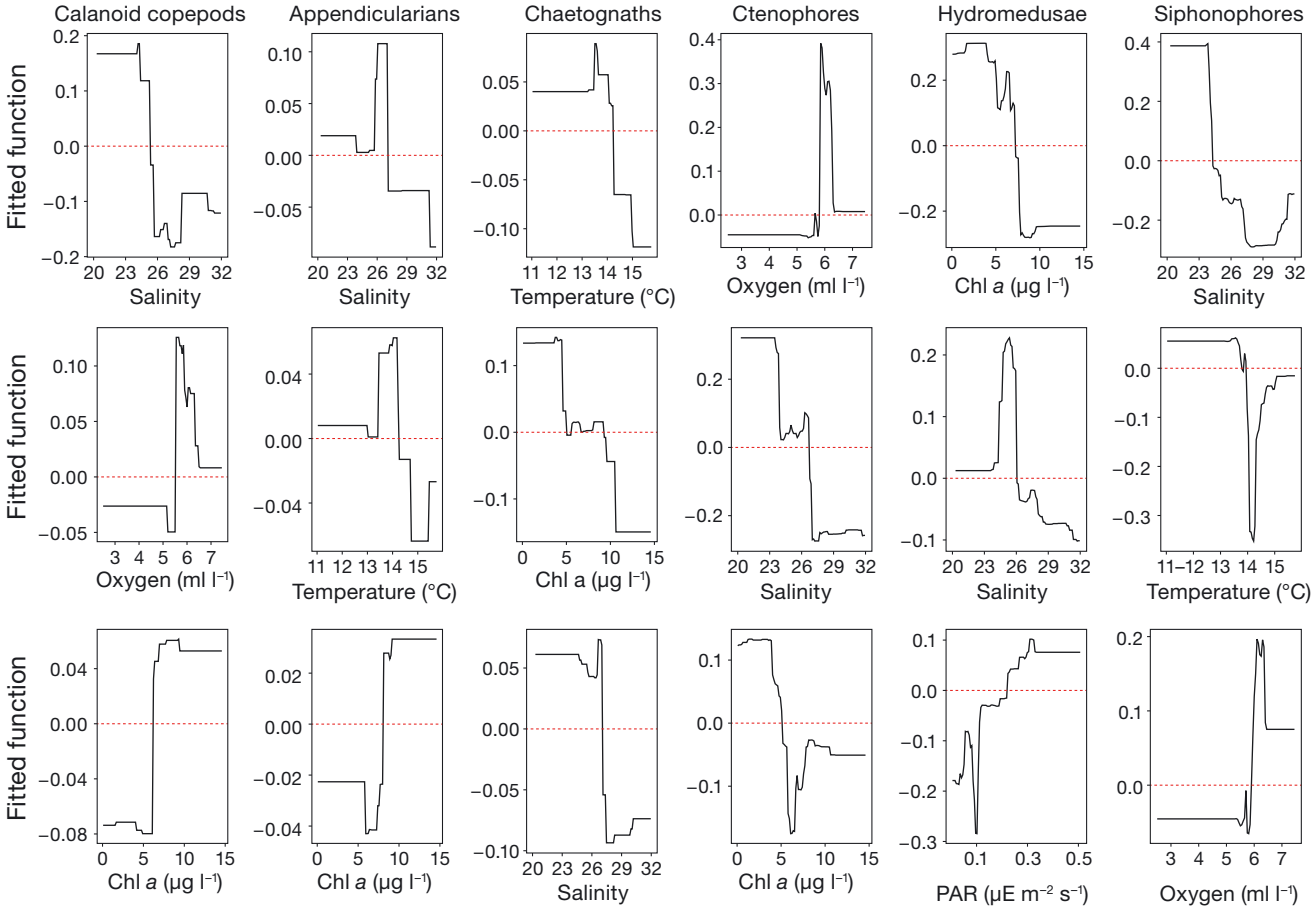

Fig. 9. Partial dependence plots of the top 3 most important explanatory variables in the likelihood of spatial overlap of larval fishes and each taxon sampled in the vicinity of the Columbia River from the boosted regression tree (BRT) analysis. Each column shows the results from a particular model and is organized in descending order of importance from top to bottom. A fitted value of 0 (red dotted line) represents a model prediction of average spatial overlap of the taxa with fish larvae; negative fitted values indicate below-average predicted overlap; positive fitted values indicate above-average predicted overlap. Chl *a*: chlorophyll *a* concentration; PAR: photosynthetically active radiation

tems such as riverine plumes, the trophic environment can quickly shift from favorable (high prey, low predator concentration) to poor (low prey, high predator concentration). Riverine plumes are important habitats for larval fishes and are thought to provide mechanisms of favorable transport (i.e. nearshore retention) and high food availability (Grimes & Finucane 1991, Govoni 1997, Eggleston et al. 1998), but traditional sampling techniques have not adequately examined the fine-scale distributions of larval fishes, their prey, and their predators in relation to highly dynamic and 3-dimensional riverine plumes. Results of our study demonstrate the effect of this dynamic physical system on the distributions and overlap of biological constituents over space (inshore versus offshore) and time (ebb versus flood tide), with potential consequences on larval fish prey/predator interactions.

4.1. Larval fish distributions

Distributions of larval fish taxa (Sebastidae, Clupeiformes, 'long slender' [possibly Bathylagidae, see Section 3.3], Pleuronectiformes, and Myctophidae) varied in space and time in both horizontal and vertical dimensions. On a broad scale, the highest concentrations of fish larvae were found in the inshore region of Transect 3, ~20 km south of the river mouth. This was consistent with expectations, as during the study period there was weak upwelling driven by northern winds that have previously been shown to divert the CRP and zooplankton southward and offshore (Hickey et al. 2005, Peterson & Peterson 2008, 2009). Further, some species, notably northern anchovy, are known to spawn in the far-field 'aged' plume waters, which may account for higher concentrations in this re-

gion compared to directly off of the river mouth (Richardson 1981, Emmett et al. 1997).

The distribution of fish larvae also changed vertically in relation to the horizontal plume front. Throughout sampling, larval fish concentrations peaked at around 10 m below the base of the plume. Although this peak was moderate in some transects, larval fishes were consistently found in higher abundances beneath fresher plume waters with negligible, near-zero concentrations within the shallow surface plume. As such, when plume waters extended deeper into the water column (Transect 2, flood tide), larval fishes were distributed deeper and appeared to be vertically compressed on short time scales (hours). Vertical plume avoidance could be due to (1) physiological limitations, (2) physical displacement, (3) biological factors, or some combination of these. Northern anchovy are euryhaline, and given that some *Sebastes* and Pleuronectiformes species use the estuary as juveniles, they may also tolerate a wide salinity range (Allen & Baltz 1997, Oh et al. 2014). However, Bathylagidae and Myctophidae are mesopelagic taxa and thus are unlikely to tolerate low salinity. Myctophidae were primarily found offshore. Our sampling did not enable us to definitively address why larval fishes were not found in surface plume waters. However, because most taxa responded to the deepening of the horizontal front in a similar manner (i.e. their distributions deepened) regardless of their varied ability to withstand a wide range of salinities, we hypothesize that physical displacement and biological factors may have played a larger role than physiological limitations in the CRP.

4.2. Fine-scale habitat partitioning beneath the plume

All prey and predator taxa were primarily distributed beneath fresher plume waters. Much like the larval fishes, vertical distributions changed with the depth of the horizontal plume front. For example, when the horizontal front extended deeper into the water column during the flood tide, all taxa were distributed at greater depths and vice versa, suggesting that broad taxa distributions were set by the physical environment, likely through density gradients or sheer at the horizontal front. Adherence of zooplankton distributions to the depth of the horizontal front due to strong density gradients has been observed in previous studies in the region (Peterson & Peterson 2008). The role of density gradients in maintaining taxa distributions is illustrated with the distribution of chaetognaths. Chaetognaths were the only taxon consistently found above negligible concentrations within the plume water at the shallowest depths. Chaetognaths are highly active ambush predators; laboratory studies found chaetognath swimming speeds to be as high as 6.2–22.5 cm s^{-1} for *Sagitta* spp., a common genus in this region (Ignatyev 1997). While these swimming speeds are similar to those of some large fish larvae, they are significantly higher than the swimming speeds attained by the relatively small fish larvae (~6 mm TL) observed in this study (Hunter 1972, Kashef et al. 2014). With strong swimming capabilities, chaetognaths may be the only taxon able to access regions above the horizontal plume front, although the advantages for doing so are unclear.

Recent *in situ* studies suggest that physical oceanographic features broadly determine the distribution of taxa, but within those distributions, zoo- and ichthyoplankton exhibit fine-scale habitat partitioning (Benoit-Bird et al. 2009, Greer et al. 2013). Concentrations of predator taxa, especially hydromedusae, peaked directly under the horizontal plume front. This is not surprising, since many of our predator groups have highly buoyant bodies that have a tendency to get 'stuck' at density discontinuities (Graham et al. 2001). Interestingly, however, the bulk of larval fishes and their prey (calanoid copepods and appendicularians) were often found below the highest peaks in predator concentrations. Further, throughout the study, fish larvae vertically overlapped with both of their prey groups, but were vertically separated from hydromedusae during both the flood tide as well as in the inshore region south of the river mouth. The vertical separation between fish larvae and hydromedusae, and simultaneous overlap with their prey, suggests that there may be some degree of habitat partitioning beneath the river plume. Although we cannot discern whether vertical spatial separation with hydromedusae and overlap with calanoid copepods and appendicularians was due to active or passive processes, we suspect that physical conditions at the horizontal front set the ultimate limits for zoo- and ichthyoplankton distributions, while beneath the plume, biological interactions acted to optimize feeding and reduce predation pressure. Given the timescale of this study (hours between Transect 1 and Transect 2), partitioning of the water column beneath the plume is unlikely to be due to the predatory 'top-down effect' of one population on another. By distinguishing patterns of different taxa on fine spatial scales, our results build upon previous findings of broad aggregations of phyto- and zooplankton near or within the density disconti-

nuity along the horizontal plume margin of the CRP (Peterson & Peterson 2008).

4.3. Trophic interactions in space and time

Based on the observed distributions and fine-scale spatial overlap of larval fishes and their prey, most fish larvae in the vicinity of the CRP should experience high concentrations of appropriately sized copepod and appendicularian prey, especially directly off of the river mouth and during the flood tide. Since calanoid copepods and appendicularians are important prey resources for larval fishes (Gadomski & Boehlert 1984, Llopiz et al. 2010, Llopiz 2013), these spatial and temporal conditions can be considered favorable feeding environments.

Potential predators were also concentrated in plume regions. Although ctenophores can be predators of larval fishes (reviewed by Purcell 1985), the ctenophores encountered in the plume regions of this study are unlikely to have functioned as prominent larval fish predators given their small mean body size compared to that of the larval fishes. The remaining predators showed some degree of vertical overlap with larval fishes in all plume regions, with the exception of hydromedusae in the flood tide and in the inshore region south of the river mouth. In the latter, fish larvae also experienced low overlap with many other predator taxa, and there was a mismatch in size with siphonophores, making trophic interactions between them and larval fishes less likely here. This lack of overlap suggests that potential predation pressure on larval fishes by a broad range of predatory taxa was reduced in the inshore region south of the river mouth relative to directly off the river mouth and offshore.

While our results indicate that larval fishes experienced the most favorable feeding conditions seaward of the river mouth, potential predation pressure (measured by fine-scale spatial overlap) in this area fluctuated on short time scales (hours) over the progression of a tidal series. Overall conditions for larval fishes may have been more favorable for survival during the flood tide when there were higher prey concentrations, higher spatial overlap of larval fishes and their prey, and reduced overlap with most of their predators, relative to during the ebb tide.

Larval fishes also experienced variable trophic environments over space. To survive, larval fishes must both find food and avoid predation and there may frequently be times where these constraints necessitate trade-offs. We hypothesize that the inshore region south of the river mouth may have provided conditions most conducive for larval survival. Although larval fish overlap with prey was substantially reduced in this region relative to near the river mouth, overlap with potential zooplanktonic predators was also lower. Considering the size of the planktonic predators in addition to overlap, chaetognaths may have been the only prominent predators of larval fishes in this region. Farther offshore, chaetognaths and ctenophores overlap with and are the appropriate size to function as predators of larval fishes. Predation is thought to be the primary agent of larval fish mortality, and baseline prey levels necessary for larval fish survival have probably been overestimated in lab-based experiments, as larvae may forage more effectively in the wild than expected (Bailey & Houde 1989). With this in mind, food availability may have been sufficiently high and predation pressure sufficiently low to sustain larval fishes nearshore south of the river mouth. This favorable trophic environment may underlie the spawning of northern anchovy in this region (Richardson 1981, Emmett et al. 1997). The degree to which such regions of potentially enhanced larval fish success are common in nearshore regions of other systems remains to be examined.

4.4. Trophic interactions and the physical environment

BRTs, which allowed us to model the relative importance of a variety of surface physical variables on the spatial overlap of larval fish and their prey/predators, revealed that surface salinity and chl *a* concentration were the most important factors influencing taxa overlap with fish larvae. Surface salinity was especially important for prey groups (calanoid copepods and appendicularians), and it was in the top 3 most important predictors for all taxa. Additional BRT analyses (not shown) incorporating subsurface data (5–10 and 20–40 m) explained less deviance than the presented top 5 m surface model.

In the CRP, the highest zooplankton abundance and biovolume were reported to occur at surface salinities of between 26 and 30, which is characteristic of the far-field 'aged' plume (Peterson & Peterson 2008, Horner-Devine et al. 2009). Our data are consistent with this pattern in that zooplankton concentrations were enhanced for many taxa within this surface salinity range. However, BRTs revealed that high zooplankton concentrations may not confer high overlap on small scales (meters in the vertical, kms in the horizontal) relevant to trophic interactions. We

found that at salinities of 27 and above, spatial overlap with fish larvae was below model average for all prey and predator taxa regardless of their high concentrations in these regions. When surface salinities were within this range, the WMD of some zooplankton was up to 30 m shallower than that of larval fishes, though this varied greatly across taxa. This fine-scale difference could explain why at even higher prey concentrations in plume-influenced waters elsewhere, larval fish had slower growth (Axler et al. 2020, this Theme Section).

Interestingly, high surface chl *a* concentrations were predicted to lead to above model average overlap of larval fishes with their prey groups, but below-average overlap with their potential predator groups. While the reasoning behind this relationship is unclear, it suggests that there are complex interactions between adjacent trophic levels in dynamic river plume systems.

4.5. River plumes as important larval fish habitats

Many species (e.g. the northern anchovy in the NCC) use river plumes as spawning and nursery habitats (Richardson 1981, Emmett et al. 1997, Parnel et al. 2008) and thus it is often assumed that plumes provide favorable conditions for the vulnerable early life stages of larval fishes. It is thought that river plumes may offer (1) nearshore retention mechanisms, (2) high food availability, and/or (3) reduced predation pressure (Grimes & Finucane 1991, Govoni 1997, Eggleston et al. 1998). Indeed, we found that river plumes provided substantially higher concentrations of prey resources and enhanced spatial coherence between larval fishes and their prey relative to oceanic waters. The functionality of river plumes as a refuge from predation was less clear. Importantly, high concentrations of larval fishes and zooplankton did not necessarily lead to high spatial overlap on fine scales (meters) relevant to larval fish trophic interactions, but these relationships were highly nuanced in space and time.

Our results help to fill gaps in our knowledge on how the physical environment can influence larval fish trophic interactions on small spatio-temporal scales. However, we also fully acknowledge the limitations of our study: this is a snapshot of a complex system, and trophic interactions are frequently species-specific. Further work would be useful to identify species-specific larval fish prey and predators in the NCC and to investigate annual variation in fine-scale larval fish prey availability and predation pressure near important habitats, like river plumes.

4.6. ISIIS and the importance of predation

High-resolution *in situ* sampling allowed us to evaluate the relationships between larval fishes, their prey, and their predators on fine spatial and temporal scales. Further, using ISIIS allowed us to explicitly investigate the role of potential predation in river plumes, an often-overlooked process determining larval fish survival. Traditional sampling techniques vastly underestimate fragile gelatinous taxa and thus the potential for predation on larval fishes. It is suggested that nets underestimate some groups of gelatinous zooplankton by 12 times (Remsen et al. 2004). Because predation may be the primary agent of larval fish mortality (Bailey & Houde 1989), understanding variations in growth, survival, and recruitment requires including accurate estimates of predation potential on fine scales.

Our sampling occurred during anomalously warm conditions in the NCC associated with a large-scale marine heatwave and El Niño forcing. This resulted in a shift in the zooplankton community from crustacean to gelatinous dominated (Brodeur et al. 2019), which likely contributed to the extremely high concentrations of some gelatinous predators observed in our sampling. Although it is difficult to say if the distributions we observed were typical for the NCC, our study certainly highlights the need for better quantification of potential predation, especially in the context of changing ocean conditions that may favor gelatinous predator taxa. This will provide a better baseline for understanding how oceanographic conditions structure fine-scale zooplankton communities, which is critical for understanding the processes that drive adult population dynamics (Houde 2008).

Acknowledgements. We thank the 3 anonymous reviewers whose comments greatly improved this manuscript. We are grateful for the opportunity to have joined the 2016 NOAA-funded pre-recruit cruise. We thank the captain and crew of the RV 'Bell M. Shimada,' as well as those involved in the shore-based operations necessary for the successful completion of this work. We are particularly indebted to Jessica Luo, Kelly Robinson, H. William Fennie, Daniel Ottmann, and Toby Auth for their contributions in the field and lab. Finally, this work could not have been completed without image processing help from Christopher Sullivan and Michaela Buchanan at Oregon State University's Center for Genomic Research and Biocomputing. While preparing this manuscript, R.K.C., S.S., M.S.S., and C.B.A. were supported by NSF OCE 1737399.

LITERATURE CITED

Acha EM, Piola A, Iribarne O, Mianzan H (2015) Ecological processes at marine fronts: oases in the ocean. Springer International Publishing, New York, NY

Albaina A, Irigoien X (2004) Relationships between frontal structures and zooplankton communities along a cross-shelf transect in the Bay of Biscay (1995 to 2003). Mar Ecol Prog Ser 284:65–75

Allen RL, Baltz DM (1997) Distribution and microhabitat use by flatfishes in a Louisiana estuary. Environ Biol Fish 50: 85–103

Alvarino A (1985) Predation in the plankton realm: mainly with reference to fish larvae. Inv Mar CICIMAR 2:1–122

Anderson MJ (2001) A new method for non-parametric multivariate analysis of variance. Austral Ecol 26:32–46

Axler KE, Sponaugle S, Hernandez F Jr, Culpepper C, Cowen RK (2020) Consequences of plume encounter on larval fish growth and condition in the Gulf of Mexico. Mar Ecol Prog Ser (in press) doi:10.3354/meps13396

Baier CT, Purcell JE (1997) Trophic interactions of chaetognaths, larval fish, and zooplankton in the South Atlantic Bight. Mar Ecol Prog Ser 146:43–53

Bailey K, Houde E (1989) Predation on eggs and larvae of marine fishes and the recruitment problem. Adv Mar Biol 25:1–83

Bakun A (2006) Fronts and eddies as key structures in the habitat of marine fish larvae: opportunity, adaptive response and competitive advantage. Sci Mar 70:105–122

Barnes C, Duxbury A, Morse B (1972) Circulation and selected properties of the Columbia River effluent at sea. In: Pruter A, Alveison D (eds) The Columbia River Estuary and adjacent ocean waters: bioenvironmental studies. University of Washington Press, Seattle, WA, p 71–80

Benoit-Bird KJ, McManus MA (2012) Bottom-up regulation of a pelagic community through spatial aggregations. Biol Lett 8:813–816

Benoit-Bird KJ, Cowles TJ, Wingard CE (2009) Edge gradients provide evidence of ecological interactions in planktonic thin layers. Limnol Oceanogr 54:1382–1392

Bezerra-Neto JF, Pinto-Coelho RM (2007) Diel vertical migration of the copepod *Thermocyclops inversus* (Kiefer, 1936) in a tropical reservoir: the role of oxygen and the spatial overlap with *Chaoborus*. Aquat Ecol 41: 535–545

Bowman M (1988) Estuarine fronts. In: Kjerfve B (ed) Hydrodynamics of estuaries. CRC Press, Boca Raton, FL, p 85–132

Brodeur RD, Auth TD, Phillips A (2019) Major shifts in pelagic micronekton and macrozooplankton community structure in an upwelling ecosystem related to an unprecedented marine heatwave. Front Mar Sci 6:212

Castro L, Cáceres M, Silva N, Muñoz M, León R, Landaeta M, Soto-Mendoza S (2011) Short-term variations in mesozooplankton, ichthyoplankton, and nutrients associated with semi-diurnal tides in a Patagonian Gulf. Cont Shelf Res 31:282–292

Cowen RK, Guigand CM (2008) *In situ* ichthyoplankton imaging system (ISIIS): system design and preliminary results. Limnol Oceanogr Methods 6:126–132

Cushing D (1990) Plankton production and year-class strength in fish populations: an update of the match/mismatch hypothesis. Adv Mar Biol 26:249–293

Eggleston DB, Armstrong DA, Elis WE, Patton WS (1998) Estuarine fronts as conduits for larval transport: hydrodynamics and spatial distribution of Dungeness crab postlarvae. Mar Ecol Prog Ser 164:73–82

Elith J, Leathwick JR, Hastie T (2008) A working guide to boosted regression trees. J Anim Ecol 77:802–813

Emmett RL, Bentley PJ, Schiewe MH (1997) Abundance and distribution of northern anchovy eggs and larvae (*Engraulis mordax*) off the Oregon coast, mid-1970s vs.1994 and 1995. In: Proceedings of the International Symposium on the Role of Forage Fishes in Marine Ecosystems. Alaska Sea Grant College Program Rep 97-01. Alaska Sea Grant College Program, Fairbanks, AK, p 505–508

Emmett RL, Brodeur RD, Miller TW, Pool SS, Krutzikowsky GK, Bentley PJ, McCrae J (2005) Pacific sardine (*Sardinops sagax*) abundance, distribution, and ecological relationships in the Pacific Northwest. Calif Coop Ocean Fish Invest Rep 46:122–143

Emmett RL, Krutzikowsky GK, Bentley P (2006) Abundance and distribution of pelagic piscivorous fishes in the Columbia River plume during spring/early summer 1998–2003: relationship to oceanographic conditions, forage fishes, and juvenile salmonids. Prog Oceanogr 68:1–26

Faillettaz R, Picheral M, Luo JY, Guigand C, Cowen RK, Irisson JO (2016) Imperfect automatic image classification successfully describes plankton distribution patterns. Methods Oceanogr 15–16:60–77

Frost BW, Bollens SM (1992) Variability of diel vertical migration in the marine planktonic copepod *Pseudocalanus newmani* in relation to its predators. Can J Fish Aquat Sci 49:1137–1141

Gadomski DM, Boehlert GW (1984) Feeding ecology of pelagic larvae of English sole *Parophrys vetulus* and butter sole *Isopsetta isolepis* off the Oregon coast. Mar Ecol Prog Ser 20:1–12

García Berdeal I, Hickey B, Kawase M (2002) Influence of wind stress and ambient flow on a high discharge river plume. J Geophys Res 107:13–24

Gorsky G, Ohman MD, Picheral M, Gasparini S and others (2010) Digital zooplankton image analysis using the ZooScan integrated system. J Plankton Res 32: 285–303

Govoni JJ (1997) The association of the population recruitment of gulf menhaden, *Brevoortia patronus*, with Mississippi River discharge. J Mar Syst 12:101–108

Govoni JJ, Chester AJ (1990) Diet composition of larval *Leiostomus xanthurus* in and about the Mississippi River plume. J Plankton Res 12:819–830

Graham B (2015) Fractional max-pooling. arXiv:1412.6071

Graham WM, Pagès F, Hamner WM (2001) A physical context for gelatinous zooplankton aggregations: a review. Hydrobiologia 451:199–212

Grantham BA, Chan F, Nielsen KJ, Fox DS and others (2004) Upwelling-driven nearshore hypoxia signals ecosystem and oceanographic changes in the northeast Pacific. Nature 429:749–754

Greenwell B, Boehmke B, Cunningham J (2019) gbm: generalized boosted regression models. R package version 2.1.5. https://cran.r-project.org/web/packages/gbm/index.html

Greer AT, Cowen RK, Guigand CM, McManus MA, Sevadjian JC, Timmerman AH (2013) Relationships between phytoplankton thin layers and the fine-scale vertical distributions of two trophic levels of zooplankton. J Plankton Res 35:939–956

Grimes CB, Finucane JH (1991) Spatial distribution and abundance of larval and juvenile fish, chlorophyll and

macrozooplankton around the Mississippi River discharge plume, and the role of the plume in fish recruitment. Mar Ecol Prog Ser 75:109–119

Henderikx Freitas F, Salidas GS, Goni M, Shearman RK, White AE (2018) Temporal and spatial dynamics of physical and biological properties along the endurance array of the California Current ecosystem. Oceanography 31:80–89

Hickey B, Pietrafesa L, Jay D, Boicourt W (1998) The Columbia River Plume study: subtidal variability in the velocity and salinity fields. J Geophys Res 103:10339–10368

Hickey B, Geier S, Kachel N, MacFadyen A (2005) A bidirectional river plume: the Columbia in summer. Cont Shelf Res 25:1631–1656

Hijmans RJ, Phillips S, Leathwick J, Maintainer JE (2017) dismo: species distribution modeling. R package version 1.1-4. https://cran.r-project.org/web/packages/dismo/dismo.pdf

Horner-Devine AR, Jay DA, Orton PM, Spahn EY (2009) A conceptual model of the strongly tidal Columbia River plume. J Mar Syst 78:460–475

Houde ED (2008) Emerging from Hjort's shadow. J Northw Atl Fish Sci 41:53–70

Hu Q, Davis C (2006) Accurate automatic quantification of taxa-specific plankton abundance using dual classification with correction. Mar Ecol Prog Ser 306:51–61

Hunter JR (1972) Swimming and feeding behavior of larval anchovy *Engraulis mordax.* Fish Bull 70:821–838

Ignatyev S (1997) Pelagic fishes and their macroplankton prey: swimming speeds. In: Proceedings of the International Symposium on the Role of Forage Fishes in Marine Ecosystems. Alaska Sea Grant College Program Rep 97-01. Alaska Sea Grant College Program, Fairbanks, AK, p 31–39

Kashef NS, Sogard SM, Fisher R, Largier JL (2014) Ontogeny of critical swimming speeds for larval and pelagic juvenile rockfishes (*Sebastes* spp., family Scorpaenidae). Mar Ecol Prog Ser 500:231–243

Lasker R (1975) Field criteria for survival of anchovy larvae: the relation between inshore chlorophyll maximum layers and successful first feeding. Fish Bull 73:453–462

LeCun Y, Bengio Y, Hinton G (2015) Deep learning. Nature 521:436–444

Lieske DJ, Schmid MS, Mahoney M (2018) Ensembles of ensembles: combining the predictions from multiple machine learning methods. In: Humphries G, Magness D, Huettmann F (eds) Machine learning for ecology and sustainable natural resource management. Springer International Publishing, Cham, p 109–121

Llopiz J (2013) Latitudinal and taxonomic patterns in the feeding ecologies of fish larvae: a literature synthesis. J Mar Syst 109–110:69–77

Llopiz JK, Cowen RK (2009) Variability in the trophic role of coral reef fish larvae in the oceanic plankton. Mar Ecol Prog Ser 381:259–272

Llopiz JK, Richardson DE, Shiroza A, Smith SL, Cowen RK (2010) Distinctions in the diets and distributions of larval tunas and the important role of appendicularians. Limnol Oceanogr 55:983–996

Lochmann S, Taggart C, Griffin D, Thompson K, Maillet G (1997) Abundance and condition of larval cod (*Gadus morhua*) at a convergent front on Western Bank, Scotian Shelf. Can J Fish Aquat Sci 54:1461–1479

Luo JY, Grassian B, Tang D, Irisson JO and others (2014) Environmental drivers of the fine-scale distribution of a gelatinous zooplankton community across a mesoscale front. Mar Ecol Prog Ser 510:129–149

Luo JY, Irisson JO, Graham B, Guigand C, Sarafraz A, Mader C, Cowen RK (2018) Automated plankton image analysis using convolutional neural networks. Limnol Oceanogr Methods 16:814–827

Mather PM (1976) Computational methods of multivariate analysis in physical geography. John Wiley & Sons, London

McClatchie S, Cowen R, Nieto K, Greer A and others (2012) Resolution of fine biological structure including small narcomedusae across a front in the Southern California Bight. J Geophys Res 117:C04020

McCune B, Grace JB (2002) Analysis of ecological communities. MJM Software Design, Gleneden Beach, OR

Möller KO, St. John M, Temming A, Floeter J, Sell AF, Hermann JP, Möllmann C (2012) Marine snow, zooplankton and thin layers: indications of a trophic link from small-scale sampling with the Video Plankton Recorder. Mar Ecol Prog Ser 468:57–69

Morgan CA, De Robertis A, Zabel RW (2005) Columbia River plume fronts. I. Hydrography, zooplankton distribution, and community composition. Mar Ecol Prog Ser 299:19–31

Munk P (2007) Cross-frontal variation in growth rate and prey availability of larval North Sea cod *Gadus morhua*. Mar Ecol Prog Ser 334:225–235

Oh SY, Kim CK, Jang YS, Choi HJ, Myoung JG (2014) Effect of salinity on survival, oxygen consumption and blood physiology of Korean rockfish *Sebastes schlegelii*. Ocean Polar Res 36:135–143

Oksanen J, Blanchet FG, Friendly M, Kindt R and others (2019) Vegan: community ecology package. R package version 2.5-6. https://cran.r-project.org/web/packages/vegan/vegan.pdf

Orenstein EC, Beijbom O, Peacock EE, Sosik HM (2015) WHOI-Plankton—a large scale fine grained visual recognition benchmark dataset for plankton classification. arXiv:1510.00745v1

Parnel MM, Emmett RL, Brodeur RD (2008) Ichthyoplankton community in the Columbia River plume off Oregon: effects of fluctuating oceanographic conditions. Fish Bull 106:161–173

Pepin P, Robert D, Bouchard C, Dower JF and others (2015) Once upon a larva: revisiting the relationship between feeding success and growth in fish larvae. ICES J Mar Sci 72:359–373

Peterson WT, Miller CB (1975) Year-to-year variations in the planktology of the Oregon upwelling zone. Fish Bull 73: 642–653

Peterson JO, Peterson WT (2008) Influence of the Columbia River plume (USA) on the vertical and horizontal distribution of mesozooplankton over the Washington and Oregon shelf. ICES J Mar Sci 65:477–483

Peterson JO, Peterson WT (2009) Influence of the Columbia River plume on cross-shelf transport of zooplankton. J Geophys Res 114:1–11

Picapedra PHS, Lansac-Tôha FA, Bialetzki A (2015) Diel vertical migration and spatial overlap between fish larvae and zooplankton in two tropical lakes, Brazil. Braz J Biol 75:352–361

Purcell J (1985) Predation on fish eggs and larvae by pelagic cnidarians and ctenophores. Bull Mar Sci 37:739–755

Purcell JE, Arai MN (2001) Interactions of pelagic cnidarians and ctenophores with fish: a review. Hydrobiologia 451: 27–44

Reiss CS, McConaugha JR (1999) Cross-frontal transport and distribution of ichthyoplankton associated with Chesapeake Bay plume dynamics. Cont Shelf Res 19:151–170

Remsen A, Hopkins TL, Samson S (2004) What you see is not what you catch: a comparison of concurrently collected net, Optical Plankton Counter, and Shadowed Image Particle Profiling Evaluation Recorder data from the northeast Gulf of Mexico. Deep Sea Res I 51:129–151

Richardson SL (1981) Spawning biomass and early life of northern anchovy, *Engraulis mordax*, in the northern subpopulation off Oregon and Washington. Fish Bull 78: 855–876

Roman M, Zhang X, McGilliard C, Boicourt W (2005) Seasonal and annual variability in the spatial patterns of plankton biomass in Chesapeake Bay. Limnol Oceanogr 50:480–492

Schmid MS, Cowen RK, Robinson K, Luo JY, Briseño-Avena C, Sponaugle S (2020) Prey and predator overlap at the edge of a mesoscale eddy: fine-scale, in-situ distributions to inform our understanding of oceanographic processes. Sci Rep 10:921

Shulzitski K, Sponaugle S, Hauff M, Walter K, D'Alessandro EK, Cowen RK (2015) Close encounters with eddies: oceanographic features increase growth of larval reef fishes during their journey to the reef. Biol Lett 11:20140746

Shulzitski K, Sponaugle S, Hauff M, Walter KD, Cowen RK (2016) Encounter with mesoscale eddies enhances survival to settlement in larval coral reef fishes. Proc Natl Acad Sci USA 113:6928–6933

Sponaugle S, Llopiz JK, Havel LN, Rankin TL (2009) Spatial variation in larval growth and gut fullness in a coral reef fish. Mar Ecol Prog Ser 383:239–249

St. John MA, MacDonald JS, Harrison PJ, Beamish RJ, Choromanski E (1992) The Fraser River plume: some preliminary observations on the distribution of juvenile salmon, herring, and their prey. Fish Oceanogr 1: 153–162

Tharwat A (2018) Classification assessment methods. Appl Comput Inf, https://doi.org/10.1016/j.aci.2018.08.003

Watanabe K, Kasai A, Antonio ES, Suzuki K, Ueno M, Yamashita Y (2014) Influence of salt-wedge intrusion on ecological processes at lower trophic levels in the Yura Estuary, Japan. Estuar Coast Shelf Sci 139:67–77

Williamson CE, Stoeckel ME (1990) Estimating predation risk in zooplankton communities: the importance of vertical overlap. Hydrobiologia 198:125–131

Editorial responsibility: Susana Garrido (Guest Editor), Lisbon, Portugal

Submitted: December 4, 2019; Accepted: May 11, 2020
Proofs received from author(s): June 16, 2020